Two Young MicroRNAs Originating from Target Duplication Mediate Nitrogen Starvation Adaptation via Regulation of Glucosinolate Synthesis in *Arabidopsis thaliana*[1][W]

Hua He, Gang Liang*, Yang Li, Fang Wang, and Diqiu Yu*

Key Laboratory of Tropical Forest Ecology, Xishuangbanna Tropical Botanical Garden, Chinese Academy of Sciences, Kunming, Yunnan 650223, China (H.H., G.L., Y.L., F.W., D.Y.); University of Chinese Academy of Sciences, Beijing 100049, China (H.H., Y.L.)

ORCID ID: 0000-0002-0622-4043 (G.L.).

Nitrogen is an essential macronutrient required for plant growth and development. A number of genes respond to nitrogen starvation conditions. However, the functions of most of these nitrogen starvation-responsive genes are unclear. Our recent survey suggested that many microRNAs (miRNAs) are responsive to nitrogen starvation in *Arabidopsis thaliana*. Here, we identified a new miRNA (miR5090) from the complementary transcript of the *MIR826* gene. Further investigation uncovered that both miRNA genes recently evolved from the inverse duplication of their common target gene, *ALKENYL HYDROXALKYL PRODUCING2* (*AOP2*). Similar to miR826, miR5090 is induced by nitrogen starvation. By contrast, the *AOP2* transcript level was negatively correlated with miR826 and miR5090 under nitrogen starvation. *GUS*-fused *AOP2* expression suggested that *AOP2* was posttranscriptionally suppressed by miR826 and miR5090. miRNA transgenic plants with significantly low *AOP2* expression accumulated fewer Met-derived glucosinolates, phenocopying the *aop2* mutants. Most glucosinolate synthesis-associated genes were repressed under nitrogen starvation conditions. Furthermore, miRNA transgenic plants with less glucosinolate displayed enhanced tolerance to nitrogen starvation, including high biomass, more lateral roots, increased chlorophyll, and decreased anthocyanin. Meanwhile, nitrogen starvation-responsive genes were up-regulated in transgenic plants, implying improved nitrogen uptake activity. Our study reveals a mechanism by which *Arabidopsis thaliana* regulates the synthesis of glucosinolates to adapt to environmental changes in nitrogen availability.

MicroRNAs (miRNAs) are a class of endogenous noncoding, small RNAs that regulate gene expression posttranscriptionally. miRNAs originate from primary miRNAs transcribed by RNA polymerase II. Dicer-like proteins in the nucleus orchestrate conversion of the primary miRNAs to precursor miRNAs and then to mature miRNAs (Chen, 2005; Voinnet, 2009). The mature miRNA duplexes are then methylated by HUA ENHANCER1 and exported to the cytoplasm by HASTY (the plant ortholog of exportin5), where they are incorporated into RNA-induced silencing complexes. In the RNA-induced silencing complex, miRNAs can either cleave the target mRNA or repress its translation through perfect, or almost perfect, complementary base pairing with its target sequences (Lu and Huang, 2008; Voinnet, 2009).

Plant miRNAs regulate many aspects of plant growth and development such as leaf morphogenesis (Palatnik et al., 2003), floral development, and the juvenile-to-adult transition (Wu et al., 2009). Recent reports revealed that several plant miRNAs are also involved in plant nutrient metabolism (Khraiwesh et al., 2012). Sulfate starvation induces miR395, which regulates sulfate assimilation and allocation by targeting *ATP SULFURYLASE*s (*APS1*, *APS3*, and *APS4*) and *SULFATE TRANSPORTER2;1* in *Arabidopsis thaliana* (Liang et al., 2010). Phosphate deficiency upregulates miR399, which controls phosphate acquisition and root-to-shoot translocation by repressing *PHOSPHATE2* (*UBIQUITIN-CONJUGATING ENZYME24*) (Chiou et al., 2006). Copper limitation induces miR397, miR398, miR408, and miR857, which regulate copper homeostasis by mediating the cleavage of genes encoding copper/zinc superoxide dismutases, copper chaperone for superoxide dismutase, and Laccases (Yamasaki et al., 2007; Abdel-Ghany and Pilon, 2008; Beauclair et al., 2010). During nitrogen deficiency, miR169 is down-regulated, whereas its targets nuclear factor Y

[1] This work was supported by the Natural Science Foundation of China [grant no. 31100186], the West Light Foundation of the Chinese Academy of Sciences, and the Chinese Academy of Sciences 135 Program [grant no. XTBG-F04].

* Address correspondence to lianggang@xtbg.ac.cn and ydq@xtbg.ac.cn.

The author responsible for distribution of materials integral to the findings presented in this article in accordance with the policy described in the Instructions for Authors (www.plantphysiol.org) is: Gang Liang (lianggang@xtbg.ac.cn).

G.L. and D.Y. conceived the project; H.H. and G.L. performed the experiments and drafted initial manuscript; Y.L. and F.W. performed the transgenic analysis; H.H., G.L., and D.Y. analyzed the data. H.H. and G.L. wrote paper.

[W] The online version of this article contains Web-only data.
www.plantphysiol.org/cgi/doi/10.1104/pp.113.228635

subunit A family members are induced. Overexpression of miR169 results in the accumulation of less nitrogen than in the wild type, suggesting a role in impairing nitrogen uptake (Zhao et al., 2011). In addition, high-throughput sequencing of *Arabidopsis thaliana* miRNAs uncovered many miRNAs responsive to different nutrient-deficient conditions (Hsieh et al., 2009; Pant et al., 2009; Liang et al., 2012).

Nitrogen is a key component of many fundamental biological molecules such as nucleic acids, amino acids, proteins, and nitrogen-containing metabolites. Thus, plants must obtain sufficient nitrogen for normal growth and development (Peng et al., 2007; Wang et al., 2012). As sessile organisms, most plants absorb nitrogen from the soil through their roots. However, there is not always sufficient nitrogen in the soil because soil erosion, rainwater leaching, and microbial consumption have removed it. To cope with this nitrogen limitation, plants have evolved sophisticated mechanisms to adapt to inhospitable environments. These adaptation mechanisms include regulating nitrogen uptake system activity and modulating root system architecture (Peng et al., 2007; Tsay et al., 2011). Nitrogen uptake by plant roots involves multiple uptake systems (Vidal and Gutiérrez, 2008; Maathuis, 2009). *Arabidopsis thaliana* primarily acquires nitrogen in the form of NO_3^- using NO_3^- transporters from the NITRATE TRANSPORTER1 (NRT1) and NRT2 families. Some of them are induced by NO_3^- to ensure increased uptake when the substrate becomes available. The plant nitrogen status also affects NO_3^- uptake, with Gln acting as a negative feedback signal (Miller et al., 2008). NH_4^+ is another form of inorganic nitrogen that is taken up by a relatively large number of high- and low-affinity NH_4^+ transporters encoded by the AMMONIUM TRANSPORTER (AMT) family (Miller et al., 2009). However, the molecular mechanisms of nitrogen sensing, the nitrogen signaling network, and the developmental responses to nitrogen limitation are not well studied.

Glucosinolates are a group of plant secondary metabolites that are largely limited to species of the order Brassicales, which include nutritionally important *Brassica* spp. crops as well as the model plant *Arabidopsis thaliana* (Wittstock and Halkier, 2002). Glucosinolates are nitrogen-rich metabolites; therefore, nitrogen availability is crucial for their synthesis. The biosynthesis of glucosinolates includes three main processes: side chain elongation of amino acids, core structure formation, and modifications of the side chain (Grubb and Abel, 2006). ALKENYL HYDROXALKYL PRODUCING2 (AOP2) is responsible for the side chain modification of Met-derived glucosinolates (Kliebenstein et al., 2001; Grubb and Abel, 2006; Neal et al., 2010). Modifications of the glucosinolate side chain are particularly important because the structure of the side chain affects the biological activity of the glucosinolates and their degradation products (Hansen et al., 2007).

Although many nitrogen starvation-responsive miRNAs have been identified (Krapp et al., 2011; Liang et al., 2012), the functions for most of them are unclear under nitrogen starvation conditions. Our previous research revealed that miR826 is significantly induced by nitrogen starvation (Liang et al., 2012). Here, a novel miRNA (miR5090) was identified from the complementary transcripts of *MIR826*. Similar to miR826, miR5090 is also up-regulated by nitrogen starvation. Further investigation suggested that both miRNAs can improve the adaptation of *Arabidopsis thaliana* to nitrogen starvation by directly affecting the synthesis of Met-derived glucosinolates.

RESULTS

Identification of a Novel miRNA in *Arabidopsis thaliana*

In our previous work (Liang et al., 2012), we used deep sequencing to analyze two small libraries derived from seedlings with or without nitrogen deprivation treatment. We found two small RNAs that completely matched with the complementary transcript (*At4g03038*) of the *MIR826* gene (*At4g03039*; Fig. 1A). This transcript was annotated as another RNA. By prediction of its RNA secondary structure, a canonical miRNA precursor stem loop structure was produced. The two small RNAs perfectly correspond to the miRNA/miRNA* (the passenger strand) complex with 2-nucleotide 3′ overhangs (Fig. 1C). We speculated that *At4g03038* is an miRNA-encoding gene. To investigate this hypothesis, we searched the Arabidopsis MPSS Plus database (http://mpss.udel.edu/at) for small RNA signatures that match with the stem loop sequence. We found that many small RNA reads are completely identical to the miR826 and mi826* sequences in the *MIR826* gene, and that many small RNA reads match with the putative miRNA and miRNA* sequence in the *At4g03038* transcript (Fig. 1B; Supplemental Fig. S1A). The combination of the stem loop structure and putative miRNA/ miRNA* sequence suggests that *At4g03038* may be an authentic *MIRNA* gene. To confirm our hypothesis, we cloned the stem loop region downstream of the *Cauliflower mosaic virus* (CaMV) 35S promoter, and performed *Agrobacterium tumefaciens*-mediated transient expression experiments in *Nicotiana benthamiana* leaves. The antisense sequence of the putative miRNA was used as a probe to detect the expression of the miRNA by northern blotting. As shown in Supplemental Fig. S1B, compared with the empty vector with no signal detected, the CaMV 35S promoter-driven stem loop sequence accumulated a high abundance of mature small RNA sequence. To determine whether the small RNA products are DICER-LIKE1 (DCL1) dependent, we detected their abundance in the *dcl1-9* mutant, revealing that these small RNAs are undetectable in the *dcl1-9* mutant compared with the wild type (Fig. 1D). Analysis of the high-throughput sequencing data deposited in the Arabidopsis MPSS Plus database revealed that both miR826 and the novel miRNA sequences were undetectable in the *dcl1-7* mutant, but were highly abundant in the wild type and *dcl2/3/4* mutant (Supplemental Fig. S1C). Therefore, our results indicate that *At4g03038* is an

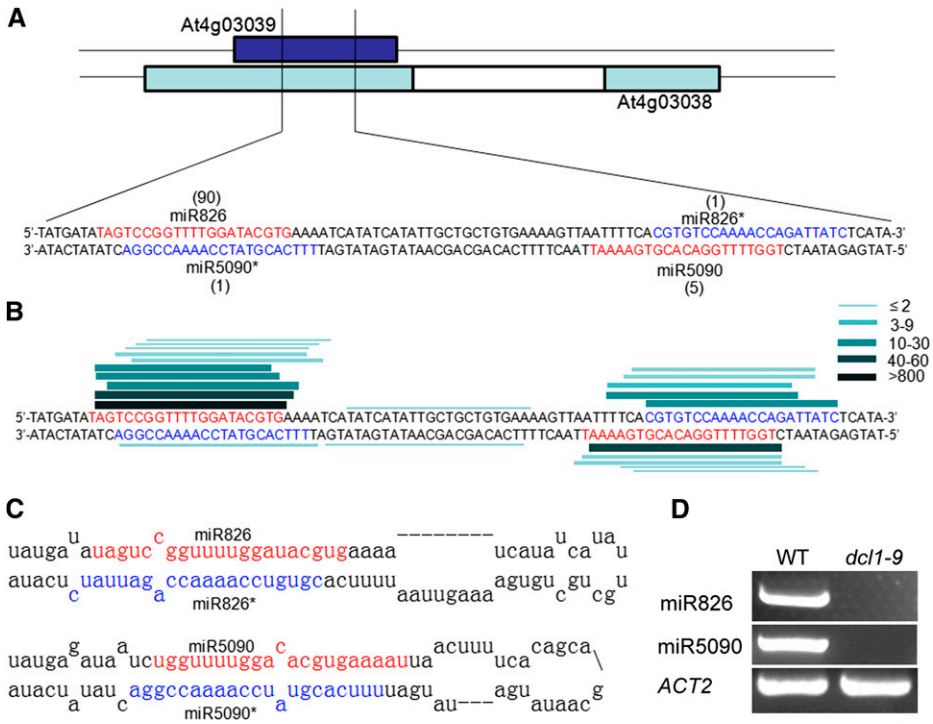

Figure 1. Identification of miR5090. A, Precursor sequences of miR826 and miR5090 with a tally of reads (from the nitrogen starvation library) mapping to the hairpins. B, Lines denote the sequences mapping to the miRNA precursors. The thickness and color of the lines correspond to the number of total reads representing each small RNA species in the Arabidopsis MPSS Plus database. C, The predicted miRNA precursors. D, RT-PCR analysis of miRNAs in the wild type (WT) and *dcl1-9* mutant.

miRNA-encoding gene. This miRNA was designated as miR5090 according to the miRNA annotation system (Ambros et al., 2003).

MIR826 and *MIR5090* Are Recently Evolved miRNAs Originating in *Arabidopsis thaliana* Genomes by Duplication of *AOP2*

miR826 was identified as a recently evolved miRNA, which is only present in *Arabidopsis thaliana*. To investigate whether miR5090 is conserved in other plant species, we searched the miRBase database (http://www.mirbase.org) for potential homologs of miR5090. However, no miR5090 homolog was found. We further searched the National Center for Biotechnology Information nucleotide database (http://blast.ncbi.nlm.nih.gov) for highly similar sequences of miR5090 by BLASTN, and found that miR5090 only matches with the *Arabidopsis thaliana AOP2* gene. Thus, the miR5090 sequence is specifically present in *Arabidopsis thaliana*. When the stem loop region sequence of miR5090 was used in a BLAST search for similar *Arabidopsis thaliana* transcripts, the only significant result was *AOP2*, which showed 89% similarity over a region of 278 nucleotides (E value = $4e^{-52}$) that extends well beyond the 21-nucleotide-long miR5090 pairing site. Target prediction (Dai and Zhao, 2011) results also indicated that *AOP2* is the candidate target of miR5090. Allen et al. (2004) suggested that new miRNAs evolve through inverted duplication of target gene sequences. Therefore, we speculated that the *MIR5090* gene originates from a duplication of its target, *AOP2*. To confirm our hypothesis, we compared the genome sequences of *AOP2* and *MIR5090*. As shown in Figure 2, six regions (F1–F6) with a high similarity (>90%) are shared by *AOP2* and *MIR5090*. Apparently, the *MIR5090* gene is a duplicate of the *AOP2* gene 3′ terminal region containing two exons and one intron. In contrast with *AOP2*, the *MIR5090* gene contains an extra inverted F5 fragment (Fig. 2), which results in the stem loop

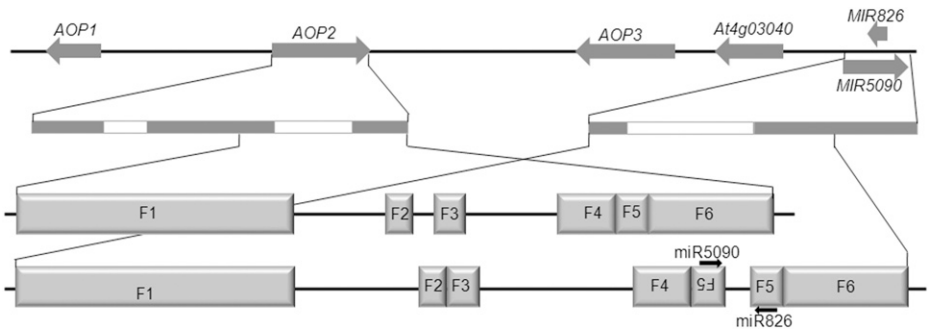

Figure 2. Extended homology between miRNA genes and the *AOP2* gene, suggestive of common origin. Three *AOP* genes and two miRNA genes are closely linked. The white bars and black bars indicate introns and exons. F1 to F6 correspond to the homologous sequences between the *AOP2* gene and the miRNA genes.

structures in miR826 and miR5090 precursors (Fig. 1C). We also compared their flanking sequences and found no significant similarity. In the *Arabidopsis thaliana* chromosome, *MIR826*, *MIR5090*, and three *AOP* genes exist in a cluster (Fig. 2). By contrast, only two *AOP* genes were found in *Arabidopsis lyrata*, from which *Arabidopsis thaliana* is thought to be derived (Yogeeswaran et al., 2005). This suggested that *MIR826* and *MIR5090* are recently evolved miRNAs.

AOP2 Is the Common Target of miR826 and miR5090

The *AOP2* gene has been identified as the target of miR826 (Rajagopalan et al., 2006; Liang et al., 2012), which encodes a 2-oxoglutarate-dependent dioxygenase that is involved in glucosinolate biosynthesis. Interestingly, target prediction results suggested that *AOP2* is also the target of miR5090. As shown in Figure 3A, the target site of miR5090 is shifted by 5 nucleotides from that of miR826. Usually, the target cleavage mediated by a plant miRNA occurs in the 10th nucleotide from the 5′ end of the miRNA (Allen et al., 2005). We identified two *AOP2* cleavage sites by a 5′ RACE experiment from nitrogen-starved *Arabidopsis thaliana* seedlings, both of which are identical to the cleavage sites retrieved from degradome data (German et al., 2008; Liang et al., 2012) and perfectly match with the 10th nucleotides of miR826 and miR5090, respectively (Fig. 3A). Thus, these two cleavage products might result from cleavage by miR826 and miR5090. To further investigate whether both miRNAs mediate the putative cleavage of *AOP2*, we performed an *Agrobacterium tumefaciens*-mediated transient assay by coexpressing the miRNA genes (*35S:MIR826* or *35S:MIR5090*) with *AOP2* (*35S:AOP2*) in *N. benthamiana* leaves. The results showed that *AOP2* mRNA levels decreased to 10% or 30% when coexpressing with miR826 or miR5090 compared with the control level, respectively (Fig. 3C). To further confirm whether the cleavage of *AOP2* occurs in the predicted target sites, several synonymous substitutions were introduced to generate miR826- and miR5090-resistant versions of *AOP2* (*35S:mAOP2*; Fig. 3B). When miR826 or miR5090 were coexpressed with *mAOP2*, the mRNA levels of *AOP2* were not affected. These results confirmed that *AOP2* is the common target of miR826 and miR5090.

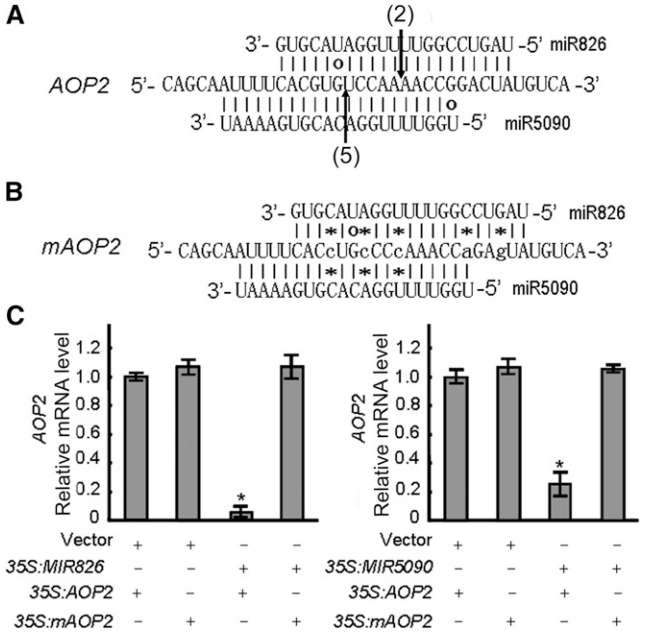

Figure 3. *AOP2* is the common target of miR826 and miR5090. A, Predicted miRNA/target duplex. Vertical arrows indicate the target cleavage positions. The number indicates the number of corresponding cleavage products from 5′ RACE experiment. B, Synonymous nucleotide substitutions in miRNA binding sites of *AOP2*. C, Cleavage of *AOP2* transcripts by miR826 and miR5090 in planta. Constructs harboring the wild type or mutated *AOP2* driven by the 35S promoter were coagroinoculated with the *35S:MIR826* or *35S:MIR5090* constructs in tobacco leaves. Empty vector was used as a negative control. Total RNAs were extracted after a 3-d inoculation and examined by qRT-PCR. The Student' *t* test indicated that the values marked by one asterisk are significantly different from the corresponding wild-type value ($P < 0.01$; n = 3).

The Transcript Abundance of miR826 and miR5090 Is Negatively Correlated with That of *AOP2* in Response to Nitrogen Starvation

We previously found that miR826 transcript abundance was particularly high in the nitrogen deprivation library, and the miR5090 transcript was only found in the nitrogen deprivation library (Liang et al., 2012). To investigate whether both miRNAs are specifically responsive to nitrogen deprivation, we tested the expressions of miR826 and miR5090 in seedlings grown under different nutrient deprivation conditions. In contrast with the slight change caused by sulfur, potassium, or phosphorus deprivation, both miR826 and miR5090 were strongly induced by nitrogen starvation (Fig. 4A), indicating that miR826 and miR5090 were specifically up-regulated by nitrogen starvation. miRNAs suppress their target transcripts; therefore, the expression of miRNAs is usually inversely correlated with that of their targets. We thus detected the transcript levels of miR826, miR5090, and *AOP2* transcripts in 10-d-old seedlings grown on medium supplemented with different nitrogen concentrations (nitrogen sufficient, 3 mM; nitrogen low, 0.3 mM; and nitrogen free, 0 mM). As expected, both miR826 and miR5090 expression levels increased with the decrease in nitrogen concentration, whereas *AOP2* showed the reverse trend (Fig. 4B). Similar results were observed when roots and shoots were examined separately (Supplemental Fig. S2). These results suggested that *AOP2* expression is negatively correlated with the expressions of miR826 and miR5090.

However, we did not know whether the reduction in *AOP2* expression directly resulted from the induction of miRNAs under nitrogen starvation conditions. To

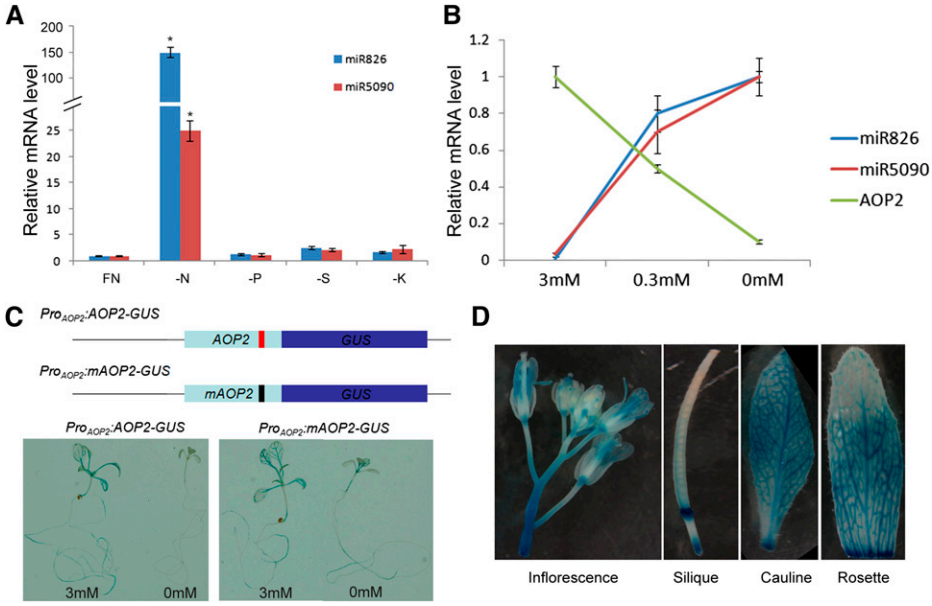

Figure 4. *AOP2* is regulated posttranscriptionally. A, Expression of miR826 and miR5090 under different nutrient deficiencies. FN, Full nutrient; K, potassium; N, nitrogen; P, phosphorus; S, sulfur. The Student's *t* test indicated that the values marked by one asterisk are significantly different from the corresponding wild-type value ($P < 0.01$; $n = 3$). B, Expressions of miRNAs and *AOP2* under nitrogen starvation. A and B, Ten-day-old seedlings were used for RNA extraction. The qRT-PCR analysis was repeated for three biological replicates, each of which consisted of three technical replicates. The error bars represent the SDS from triplicate samples. C, GUS staining under nitrogen starvation conditions. The scheme represents two reporters with wild-type or mutated *AOP2*. Ten-d-old seedlings were used for GUS staining. D, GUS staining under different tissues and organs. The 2-month-old *Pro$_{AOP2}$:AOP2-GUS* reporter line was used for GUS staining.

uncover the regulation of *AOP2* by miRNAs, we prepared two reporters. First, the wild-type *AOP2* complementary DNA (cDNA) was fused in frame with a *GUS* gene driven by the 2.9-kb genomic region upstream of the start codon of *AOP2* (Fig. 4C). This wild-type reporter (*Pro$_{AOP2}$:AOP2-GUS*) would allow us to monitor *AOP2* transcriptional and posttranscriptional regulation. In agreement with the quantitative reverse transcription PCR (qRT-PCR) results, *Pro$_{AOP2}$:AOP2-GUS* was strongly expressed in roots and shoots under nitrogen-sufficient conditions, whereas GUS staining was very weak under nitrogen-free conditions (Fig. 4C). To reveal the effect of miRNAs on the expression of *AOP2*, we prepared a second reporter, with mutated *AOP2* (*mAOP2*) (Fig. 4C). Compared with nitrogen-sufficient conditions, the expression of *Pro$_{AOP2}$:mAOP2-GUS* was down-regulated only moderately under nitrogen-free conditions (Fig. 4C). GUS staining in the whole plant indicated that *AOP2* was ubiquitously expressed in inflorescence, silique, cauline, and rosette leaves (Fig. 4D). These results demonstrated that under nitrogen starvation, the expression of *AOP2* is suppressed by miRNAs at the posttranscriptional level.

Overexpression of miR826 or miR5090 Suppresses the Accumulation of the *AOP2* Transcript

To further understand the functions of miR826 and miR5090, we generated transgenic plants overexpressing miR826 or miR5090. Twelve and eight independent transgenic lines for *35S:MIR826* and *35S:MIR5090* were obtained, respectively. We determined the miRNA expression levels of five independent lines for each genotype. The antisense DNA sequences of the two miRNAs were labeled with ^{32}P and used as probes to detect the expression of these two miRNAs using northern blotting. Compared with the wild type, all of the transgenic plants we examined produced high quantities of mature miRNAs (Fig. 5A). Further analysis suggested that *AOP2* transcript levels were dramatically down-regulated in the transgenic plants (Fig. 5B). When subjected to different nitrogen starvation conditions, the transcript abundance of *AOP2* in transgenic plants remained low compared with the wild type (Fig. 5B). The overproduction of miR826 or miR5090 correlated well with the decreased *AOP2* mRNA level in transgenic plants, suggesting that miR826 and miR5090 suppress *AOP2* mRNA abundance.

Transgenic Plants Mimic the Phenotypes of *aop2* Mutants

The *AOP2* gene displays polymorphism across different *Arabidopsis thaliana* ecotypes (Kliebenstein et al., 2001). The ecotype Cape Verde Islands of *Arabidopsis thaliana* (Cvi) contains a functional *AOP2* gene, whereas ecotype Columbia of *Arabidopsis thaliana* (Col) has a nonfunctional *AOP2* gene resulting from a 5-bp

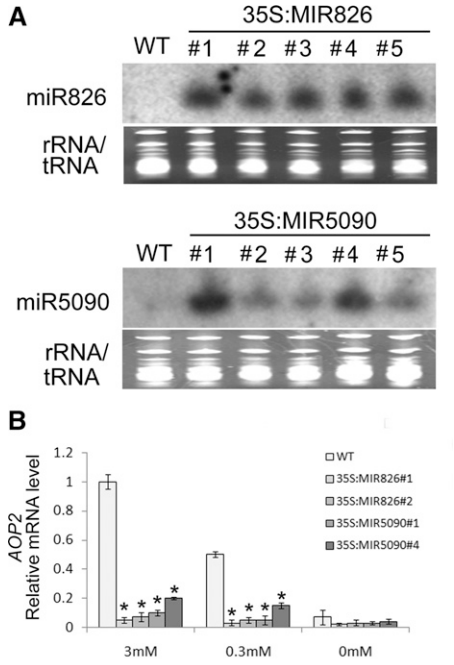

Figure 5. Expressions of miR826, miR5090, and *AOP2* in wild-type (WT) and transgenic plants. A, Leaves from 4-week-old plants were used for RNA extraction. Ribosomal RNA/tRNA staining is shown as a loading control. Twenty micrograms of total RNA was used for northern blotting. Numbers 1 to 5 represent different transgenic lines. B, Expression of *AOP2*. Plants were grown for 10 d on MS medium with the indicated nitrogen concentrations. RNA was isolated from whole seedlings. The qRT-PCR analysis was repeated for three biological replicates, each of which consisted of three technical replicates. The error bars represent the SDS from triplicate samples. A Student's *t* test indicated that the values marked by one asterisk are significantly different from the corresponding wild-type value ($P < 0.01$; $n = 3$).

deletion in its transcript. Therefore, all our experiments are performed in the Cvi ecotype. Given the significant reduction of *AOP2* in transgenic plants, we expected that they could mimic the glucosinolate profiles of Col ecotype plants that contain a mutated *aop2*. Thus, we detected the glucosinolate profiles in miR826 and miR5090 transgenic plants to determine whether the composition of the glucosinolates had changed as a result of the down-regulation *AOP2* expression. As shown in Figure 6, Cvi contains AOP2-catalyzed products 2-propenyl (7.7 min; peak 3) and 3-butenyl (12.2 min; peak 4) glucosinolates. By contrast, Col (a natural *aop2* mutant) accumulated 3-methylsulfinylpropyl (5.2 min; peak 1) and 4-methylsulfinylbutyl (7.0 min; peak 2) glucosinolates, both of which are the substrates of AOP2 (Fig. 6). We then detected the glucosinolate profiles of miR826 and miR5090 transgenic plants: High levels of 3-methylsulfinylpropyl and 4-methylsulfinylbutyl glucosinolates, but not AOP2-catalyzed products, were detected. These results suggested that elevated miR826 or miR5090 expression suppresses the function of *AOP2*, resulting in the reduction of Met-derived glucosinolates.

Altered Expression of Genes Involved in Aliphatic Glucosinolate Synthesis

Glucosinolate biosynthesis involves three stages: 1) chain elongation of selected precursor amino acids (only Met and Phe), 2) formation of the core glucosinolate structure, and 3) secondary modifications of the amino acid side chain (Sønderby et al., 2010). AOP2 is a key regulator for glucosinolate synthesis, which is responsible for the secondary modifications of Met-derived glucosinolates that are the major components of aliphatic glucosinolates. Considering the down-regulation of *AOP2* under nitrogen starvation conditions, we asked whether glucosinolate synthesis-associated genes would be affected by nitrogen starvation. Among the 31 genes (Table I), 19 decreased by 35% in the wild type under nitrogen-free conditions compared with that under nitrogen-sufficient conditions.

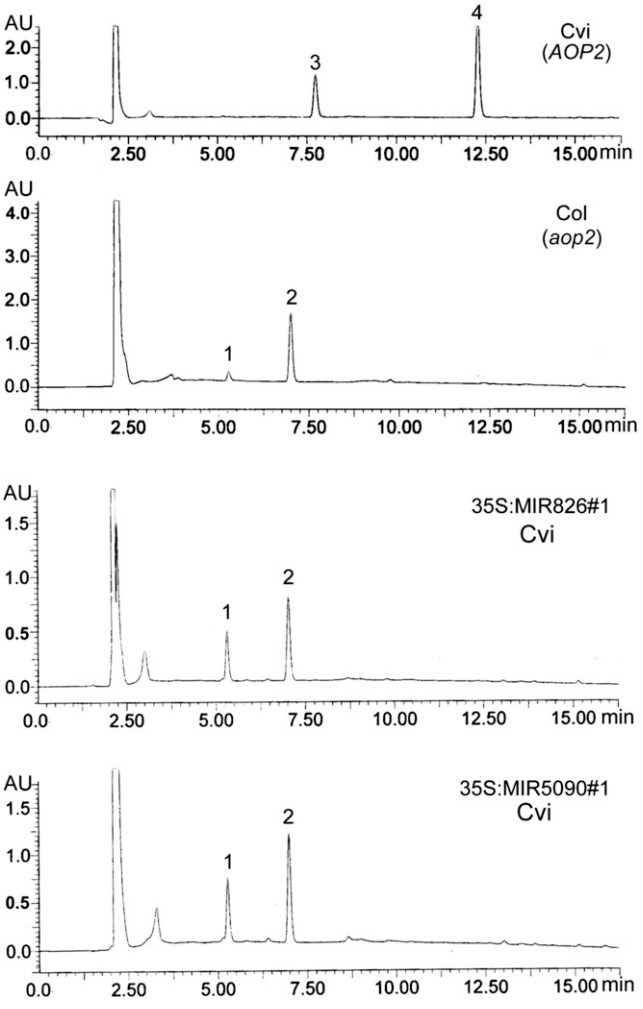

Figure 6. UPLC profile of glucosinolates from different plants. Peak 1 corresponds to 3-methylsulfinylpropyl glucosinolate. Peak 2 corresponds to 4-methylsulfinylbutyl glucosinolate. Peak 3 corresponds to 2-propenyl glucosinolate. Peak 4 corresponds to 3-butenyl glucosinolate.

Under both nitrogen-sufficient and nitrogen-deficient conditions, the down-regulated genes by nitrogen starvation always kept at lower levels in miRNA transgenic plants compared with the wild type. It suggested that both nitrogen starvation and *AOP2* reduction caused down-regulation of glucosinolate synthesis-associated genes.

miRNA Transgenic Plants Display Enhanced Tolerance to Nitrogen Starvation

Considering the fact that miR826 and miR5090 are induced by nitrogen starvation, we asked whether they are involved in regulating the adaptation of *Arabidopsis thaliana* to nitrogen deficiency. Under nitrogen starvation conditions, plants often show physiological and developmental adaptation such as small stature, decreased primary root length, increased lateral root density, higher anthocyanin accumulation, and lower chlorophyll content (Maathuis, 2009; Tsay et al., 2011). Therefore, we evaluated the response of miRNA transgenic plants to nitrogen starvation. Wild-type and transgenic plants, which were grown on nitrogen-sufficient, nitrogen-low, and nitrogen-free agar medium, respectively, for 10 d, were used for the analysis. Under nitrogen-sufficient and nitrogen-low conditions, the fresh weight of transgenic plants was higher than that of the wild type (Fig. 7A). Although wild-type and transgenic plants displayed similar root systems under nitrogen-sufficient conditions, the transgenic plants generated longer primary roots and higher lateral root density than the wild type under nitrogen-low conditions (Fig. 7, B and C; Supplemental Fig. S3). With the reduction of nitrogen concentration, all plants produced more anthocyanin. However, under nitrogen-sufficient and nitrogen-low conditions, the anthocyanin concentration of transgenic plants was lower than in the

Table I. *Relative expression of genes involved in aliphatic glucosinolate pathway*

Gene Name	Gene Accession	Nitrogen-Sufficient Condition (3 mM)			Nitrogen-Low Condition (0.3 mM)			Nitrogen-Free Condition (0 mM)		
		Wild Type	35S:MIR5090	35S:MIR826	Wild Type	35S:MIR5090	35S:MIR826	Wild Type	35S:MIR5090	35S:MIR826
Side-chain elongation										
BCAT3	AT3G49680	1.00	0.97	0.70	0.93	0.76	0.68	0.85	0.78	0.65
BCAT4	AT3G19710	1.00	0.97	0.56	0.80	0.40	0.50	0.32	0.11	0.10
BAT5	AT4G12030	1.00	1.02	0.84	0.93	0.60	0.80	0.50	0.31	0.24
LeuC	AT4G13430	1.00	0.90	0.73	1.25	0.87	0.77	0.90	0.67	0.61
LeuD1	AT2G43100	1.00	0.37	0.55	0.79	0.59	0.80	0.47	0.31	0.29
LeuD2	AT3G58990	1.00	1.00	0.67	1.06	0.79	0.77	0.61	0.51	0.33
IPMDH1	AT5G14200	1.00	1.02	0.63	0.87	0.61	0.66	0.47	0.36	0.25
IPMDH2	AT1G80560	1.00	0.69	0.69	0.99	1.08	1.21	0.91	0.89	1.07
IPMDH3	AT1G31180	1.00	0.59	0.41	0.91	0.63	0.74	0.62	0.33	0.43
MAM1	AT5G23010	1.00	0.73	0.51	0.68	0.43	0.55	0.60	0.18	0.12
MAM3	AT5G23020	1.00	0.13	0.17	0.19	0.14	0.11	0.41	0.16	0.18
Core structure										
CYP79F1	AT1G16410	1.00	0.91	0.65	0.74	0.56	0.59	0.46	0.17	0.19
CYP79F2	AT1G16400	1.00	0.79	0.68	0.98	0.88	0.98	0.74	0.39	0.42
CYP83A1	AT4G13770	1.00	0.75	0.53	0.84	0.52	0.47	0.59	0.26	0.24
GSTF11	AT3G03190	1.00	0.91	0.79	0.95	0.62	0.77	0.37	0.25	0.26
GSTU20	AT1G78370	1.00	0.61	0.44	0.59	0.30	0.37	0.24	0.16	0.16
GGP1	AT4G30530	1.00	0.81	0.67	1.19	1.80	1.07	1.63	1.80	1.57
SUR1	AT2G20610	1.00	0.68	0.58	1.02	1.17	0.73	0.84	1.06	0.84
UGT74C1	AT2G31790	1.00	1.00	0.63	1.10	0.65	0.77	0.70	0.55	0.64
ST5b	AT1G74090	1.00	0.94	0.80	1.02	0.83	0.66	0.76	0.72	0.57
ST5c	AT1G18590	1.00	0.93	0.56	0.86	0.61	0.61	0.48	0.40	0.39
Secondary modification										
FMOGX-OX1	AT1G65860	1.00	1.31	0.89	0.86	0.78	0.87	0.84	0.49	0.39
FMOGX-OX2	AT1G62540	1.00	1.53	1.08	2.32	1.94	2.95	2.97	2.24	4.23
FMOGX-OX3	AT1G62560	1.00	1.02	0.87	0.91	0.68	0.87	0.57	0.24	0.20
FMOGX-OX4	AT1G62570	1.00	1.01	0.92	1.98	2.70	2.67	7.37	5.98	5.35
FMOGX-OX5	AT1G12140	1.00	1.04	0.88	1.70	1.70	1.88	2.55	2.40	2.53
GS-OH	AT4G03060	1.00	0.73	0.81	0.67	0.36	0.26	0.24	0.20	0.10
AOP2	AT2G25450	1.00	0.26	0.03	0.50	0.20	0.02	0.31	0.08	0.01
Transcription factor										
MYB28	AT5G61420	1.00	1.48	1.19	0.78	0.54	0.86	1.00	0.90	0.65
MYB29	AT5G07690	1.00	1.09	0.78	0.84	0.59	0.61	0.39	0.19	0.16
MYB76	AT5G07700	1.00	0.93	0.80	0.61	0.32	0.36	0.27	0.24	0.10
Unknown factor										
AOP1		1.00	0.52	0.21	0.85	0.44	0.20	0.57	0.32	0.19

wild type (Fig. 7D). By contrast, nitrogen starvation resulted in the reduction of chlorophyll concentration in all plants; however, under nitrogen-sufficient and nitrogen-low conditions, more chlorophyll was produced in the transgenic plants compared with the wild type (Fig. 7E). These results revealed that miRNA transgenic plants display enhanced tolerance to nitrogen limitation conditions, although no significant phenotypic difference was observed between wild-type and transgenic plants under nitrogen-free conditions. To determine whether transgenic plants were also tolerant to long-term nitrogen starvation, plants were grown on agar medium for 3 weeks. As shown in Figure 7F, wild-type plants generated more senescent leaves than transgenic plants under nitrogen-sufficient conditions. By contrast, transgenic plants were significantly bigger under nitrogen-low conditions than the wild type, despite similar senescent symptoms. We also determined the phenotypes of plant grown in soil and found that transgenic plants had a higher growth rate than wild-type plants (Supplemental Fig. S4). Total nitrogen measurement revealed that individual transgenic plants contained more nitrogen than individual wild-type plants, although their nitrogen concentrations were similar in both roots and shoots (Supplemental Fig. S5).

Altered Responses to Nitrogen Limitation in Transgenic Plants

Considering the high biomass and lateral root density of transgenic plants, we speculated that transgenic plants might facilitate nitrogen uptake by the roots. An NO_3^--triggered signaling pathway stimulates elongation of growing lateral roots (Zhang and Forde, 1998). This mechanism involves three genes: *ARABIDOPSIS NITRATE-REGULATED1* (*ANR1*; Zhang and Forde, 1998), *NRT1.1*, and *NRT2.1* (Remans et al., 2006a, 2006b). Expression analysis indicated that these genes were upregulated in transgenic plants under nitrogen-sufficient conditions (Fig. 8, A and C). Under nitrogen-low conditions, the enhanced lateral root systems (Fig. 7C; Supplemental Fig. S3) of the transgenic plants correlated well with the elevated expression of *ANR1* (Fig. 8A). NO_3^- and NH_4^+ are the two main forms of nitrogen nutrients in soils absorbed by plant roots. NRT2 transporters are responsible for NO_3^- uptake (Miller et al., 2009). Our results revealed that *NRT2.1* expression was increased in transgenic plants under nitrogen-sufficient and nitrogen-low conditions (Fig. 8C), implying a stimulated nitrogen uptake activity. NH_4^+ uptake is attributed to AMT-type transporters (Yuan et al., 2007; Miller et al., 2009). We determined the expressions of *AMT1.1*,

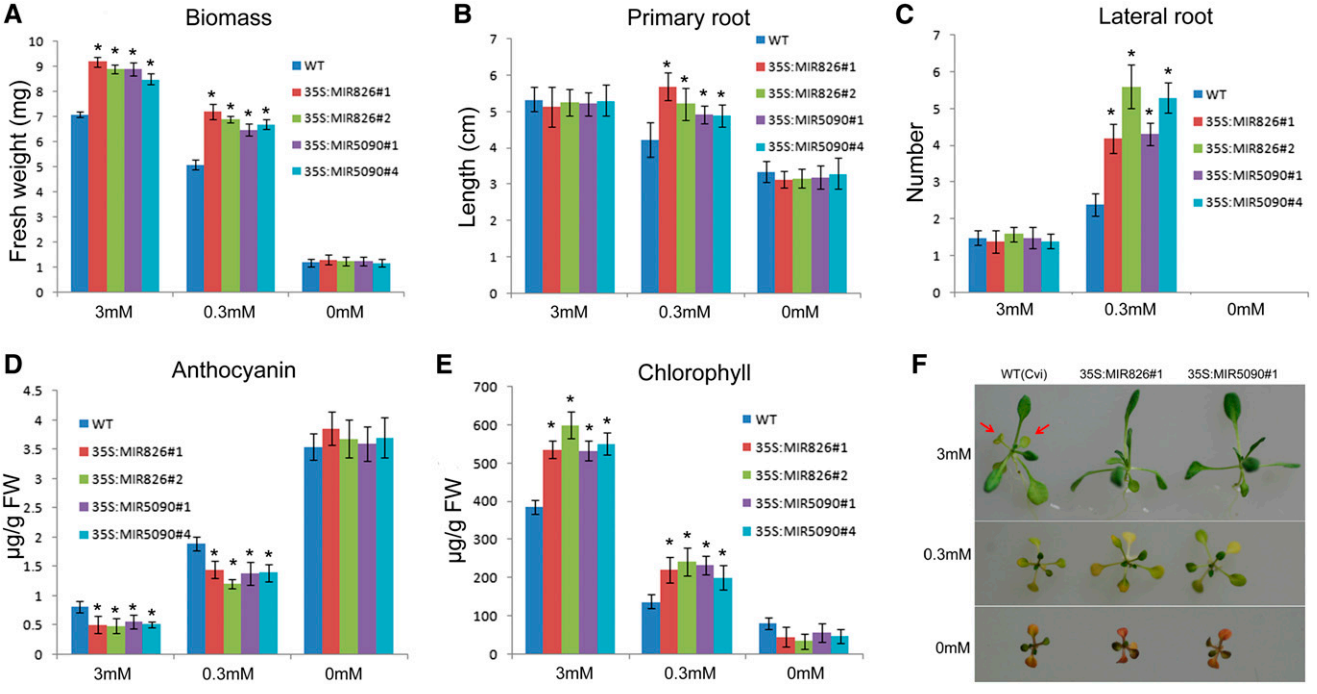

Figure 7. Transgenic plants are less sensitive to nitrogen starvation. A, Biomass. Values are the means of three replicates of 20 plants. B, Primary root length. C, Lateral root density. D, Anthocyanin concentration. Shoots were harvested for analysis. E, Chlorophyll concentration. Shoots were harvested for analysis. A to E, Ten-d-old plants grown on plates were used for analysis. Error bars indicate the SDS ($n = 3$). Asterisks indicate statistical significance at $P < 0.01$ compared with the wild type (Student's t test). F, Three-week-old seedlings grown on medium with the indicated nitrogen concentrations.

AMT1.2, and *AMT1.5* (Fig. 8, D to F), demonstrating that only *AMT1.5* was up-regulated in transgenic plants. Taken together, our results suggested that the nitrogen uptake system in transgenic plants may be improved, leading to enhanced tolerance to nitrogen limitation.

DISCUSSION

Mineral nutrients are vital to plant growth and thus affect crop yield. Several miRNAs involved in nutrient homeostasis have been characterized such as miR169 for nitrogen (Zhao et al., 2011), miR395 for sulfur (Liang et al., 2010), miR397, miR398, miR408, and miR857 for copper (Abdel-Ghany and Pilon, 2008), miR399 for phosphorus (Chiou et al., 2006), and miR827 for nitrogen and phosphorus (Kant et al., 2011). Nitrogen, one essential macronutrient for plant growth, is often deficient in the environment where plants grow. Our previous research showed that many plant miRNAs are responsive to nitrogen starvation, among which miR826 was dramatically induced by nitrogen starvation (Liang et al., 2012). Here, we identified a novel miRNA gene (*MIR5090*) from the complementary transcript of *MIR826*. Like miR826, miR5090 was also significantly up-regulated by nitrogen starvation. Our results revealed that both miR826 and miR5090 regulate the adaptation of *Arabidopsis thaliana* to low nitrogen conditions by affecting glucosinolate synthesis.

MIR826 and *MIR5090* Have Recently Evolved from Their Common Target, *AOP2*

More than 300 miRNAs were identified in *Arabidopsis thaliana* (miRBase database; http://www.mirbase.org), approximately one third of which are conserved across plant species. Generally, a conserved miRNA family contains more than one member. By contrast, there is only one member for miR826 and miR5090 families in *Arabidopsis thaliana*, implying that they are nonconserved miRNAs. In contrast with conserved miRNAs, miR826 and miR5090 are only identified in *Arabidopsis thaliana*. We could not find their potential orthologs in *Arabidopsis lyrata*, which shares over 80% of its miRNA genes with *Arabidopsis thaliana* (Fahlgren et al., 2010), implying that they are recently evolved miRNAs. To date, two hypotheses for the origins of miRNA have been proposed: One is the inverted duplication of the target (Allen et al., 2004), and the other is random sequence origin (Felippes et al., 2008). The DNA fragment containing the *MIR826* and *MIR5090* genes displays high similarity to the *AOP2* gene (Fig. 2), indicating that they are evolved from an inverted duplication of the *AOP2* sequence. Further sequence analysis revealed that a short DNA fragment (34 bp) is inversely duplicated, which contains the stem loop structure of two RNA transcripts (Pri-miR826 and Pri-miR5090). Three *AOP* genes are

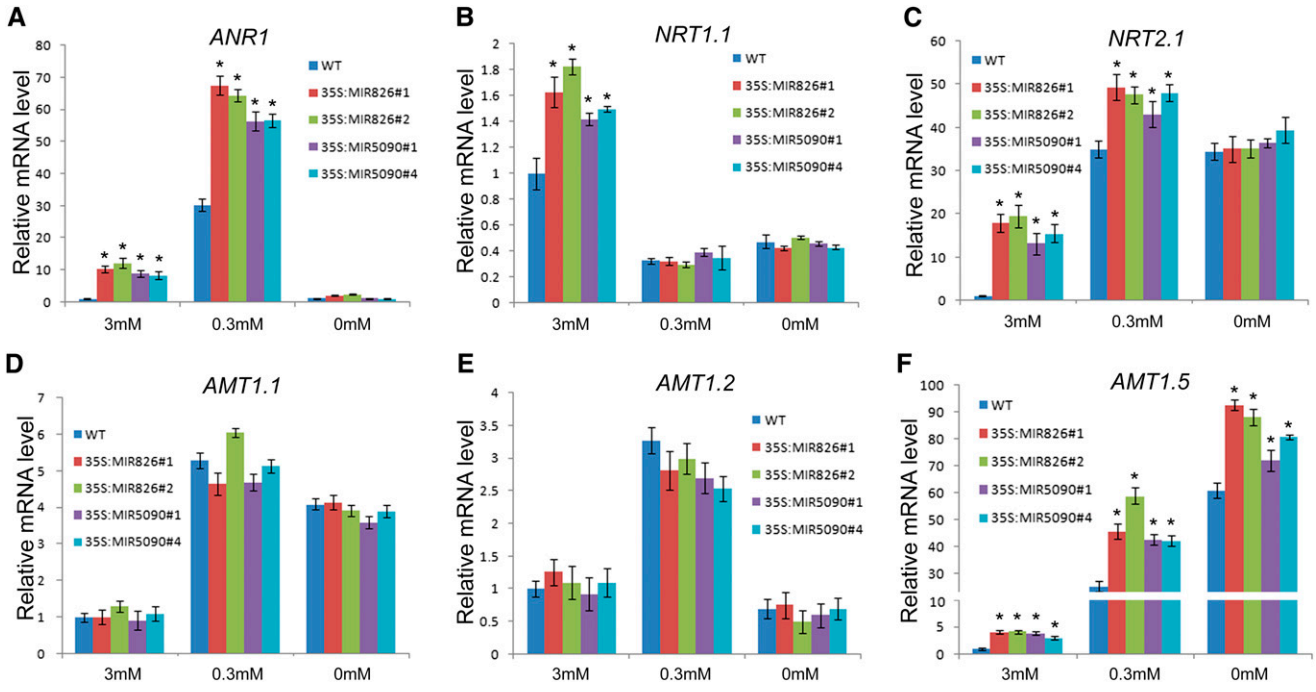

Figure 8. Expression of nitrogen starvation-responsive genes. Roots of 10-d-old plants were used for expression analysis of *ANR1* (A), *NRT1.1* (B), *NRT2.1* (C), *AMT1.1* (D), *AMT1.2* (E), and *AMT1.5* (F). The qRT-PCR analysis was repeated for three biological replicates, each of which consisted of three technical replicates. The error bars represent the SDS from triplicate samples. The Student's *t* test indicated that the values marked by one asterisk are significantly different from the corresponding wild-type value ($P < 0.01$; $n = 3$).

located in the same chromosome in a tandem manner in the Col ecotype (Fig. 2). The ecotype Landsberg *erecta* of *Arabidopsis thaliana* contains two *AOP1* genes (*AOP1.1* and *AOP1.2*) and one *AOP3*, but no *AOP2*. Both Col and Cvi contain one *AOP1* gene and one *AOP3* gene (in both ecotypes, *AOP3* is transcriptionally silent due to natural variation; Kliebenstein et al., 2001). Thus, a recent local genome rearrangement event has caused the tandem repeat of *AOP* genes in *Arabidopsis thaliana*. Over time, mutational drift would lead to erosion of the extended similarities between the originating locus and the inverted repeat. However, the sequences of the *MIR826* and *MIR5090* genes show high similarity to a 3′ fragment of the *AOP2* gene, implying that these two miRNAs evolved very recently. A similar example is the *Arabidopsis thaliana*-specific young miRNAs, miR161 and miR163, both of which are physically linked to their target loci and retain extended complementarity (Allen et al., 2004). Therefore, *MIR826* and *MIR5090* have recently evolved from the duplication of *AOP2* genomic 3′ fragment.

AOP2 Is Down-Regulated by Nitrogen Starvation via miR826 and miR5090

As a suppressor of target genes, miRNAs often mediate the cleavage of their target transcripts (i.e. regulation occurs at the posttranscriptional level; Voinnet, 2009). Target prediction indicated that *AOP2* is the common target of miR826 and miR5090. Our transient expression experiment revealed that both miRNAs are able to mediate the cleavage of *AOP2* mRNAs. Moreover, the cleavage positions in *AOP2* transcripts perfectly match with the predicted miRNA cleavage sites. When nucleotide mutations were introduced into the miRNA recognition sites, the mutated *AOP2* mRNA became insensitive to miR826 and miR5090, suggesting that sequence complementarity of target sites are crucial for the regulation of *AOP2* by miRNAs.

miRNA expression is inversely correlated with the expression of its target, unless that the miRNA and its target are expressed in different tissues or cell compartments (Voinnet, 2009). Upon a decrease in nitrogen concentration, expressions of miR826 and miR5090 were up-regulated, whereas *AOP2* expression was down-regulated. This negative correlation implies that *AOP2* expression is spatiotemporally consistent with its suppressors (miR826 and miR5090). The GUS reporter indicated that *AOP2* is ubiquitously expressed in the whole plant (Fig. 4D). GUS expression from the wild-type reporter (Pro_{AOP2}:*GUS-AOP2*) was significantly repressed by nitrogen starvation, whereas that of mutated reporter (Pro_{AOP2}:*GUS-mAOP2*) was less affected by nitrogen starvation, indicating that *AOP2* is suppressed by miR826 and miR5090 at the posttranscriptional level.

The genes from the same family are often targeted by miRNAs from different families. For example, miR160 and miR167 target *ARF* genes (Wang et al., 2005; Yang et al., 2006); miR397, miR408, and miR857 target *Laccase* genes (Abdel-Ghany and Pilon, 2008); and miR168 and miR403 target *AGO* genes (Allen et al., 2005). However, it does not happen frequently that one gene is targeted by more than one miRNA. In *Arabidopsis thaliana*, the *CHX18* gene is targeted by miR780 and miR856 (Fahlgren et al., 2007). Jeong et al. (2011) demonstrated that miR156a and miR529a target *SPL14* in rice (*Oryza sativa*). Our study established that miR826 and miR5090 can target the same target (*AOP2*). These two miRNAs may have different functions under different conditions, because, in addition to nitrogen starvation, the expression of *AOP2* is also affected by light and dark (Neal et al., 2010). Alternatively, these two recently evolved miRNAs are currently undergoing evolutionary selection. As revealed by Fahlgren et al. (2007), *MIRNA* genes undergo relatively frequent birth and death, with only a subset being stabilized by integration into regulatory networks.

Overexpression of miR826 and miR5090 Results in Reduced Accumulation of Met-Derived Glucosinolates

Our results suggested that *AOP2* is the common target of miR826 and miR5090. Compared with wild-type plants, *AOP2* in miR826 and miR5090 transgenic plants is strongly down-regulated, regardless of the nitrogen status of the environment. Hence, it is expected that transgenic plants can phenocopy *aop2* mutants. AOP2 functions in the side chain modification of Met-derived glucosinolates (Kliebenstein et al., 2001; Neal et al., 2010). Loss of function of *AOP2* led to considerably lower accumulation of Met-derived glucosinolates than in an *Arabidopsis thaliana* ecotype with one functional *AOP2* allele (Kliebenstein et al., 2001; Wentzell et al., 2007). Our results also confirmed that *aop2* mutant accumulates much less alkenyl glucosinolates (Met-derived glucosinolates; Fig. 6). As expected, miRNA transgenic plants have a very similar glucosinolate profile to *aop2* mutants. Therefore, overexpression of miRNAs is sufficient to reduce the accumulation of Met-derived glucosinolates. Our work provides a molecular tool for breeding of *Brassica* spp. vegetable crops with decreased levels of Met-derived glucosinolates, which has implications for production of functional foods enriched with particular glucosinolates.

Loss of Function of *AOP2* Causes Improved Nitrogen Starvation Adaptation in *Arabidopsis thaliana*

In our nitrogen starvation adaptation experiments, transgenic plants displayed significant growth advantages compared with the wild type. Corresponding to the phenotypes, the expressions of nitrogen starvation-responsive genes were altered in transgenic plants (Fig. 8). The increases in the expressions of nitrogen starvation-responsive genes may stimulate nitrogen uptake abilities of transgenic plants because the total nitrogen amount of individual transgenic plants was

higher than that of individual wild-type plants (Supplemental Fig. S5). Under nitrogen-sufficient conditions, no morphological difference was observed for the roots of transgenic plants and the wild type. By contrast, under the nitrogen-low conditions, transgenic plants had longer primary roots and more lateral roots than the wild type. In agreement with root phenotypes, *NRT2.1*, a key regulator in root development under nitrogen-limited conditions (Remans et al., 2006b), increased in transgenic plants compared with the wild type. Therefore, in addition to the increased expression of nitrogen transporters, transgenic plants also enhanced their root systems for adaptation to nitrogen-low conditions. Despite having the same origin, the mature sequence of miR826 is different from that of miR5090. However, miR826 transgenic plants displayed phenotypes nearly identical to that of miR5090 transgenic plants. The only common feature for miR826 and miR5090 is that they have the same target gene, *AOP2*. Therefore, loss of function of *AOP2* in transgenic plants causes the enhanced adaptation to nitrogen starvation. As a key enzyme in glucosinolate synthesis, AOP2 is the major regulator for aliphatic glucosinolate accumulation (Wentzell et al., 2007). An *AOP2* null variant shows up to 3-fold fewer aliphatic glucosinolates compared with the functional *AOP2* variant (Kliebenstein et al., 2001). In miRNA transgenic plants, the function of *AOP2* was dramatically suppressed, which may reduce the consumption of nitrogen used for glucosinolate synthesis, thereby increasing the synthesis of nitrogen-containing metabolites that are necessary for plant growth and development under nitrogen starvation conditions. Meanwhile, nitrogen is one of the major components that are integrated into glucosinolates; therefore, it is possible that the reduction of glucosinolates promotes plants to acquire more nitrogen to meet the demand of glucosinolate synthesis. Correspondingly, nitrogen starvation also repressed most glucosinolate synthesis-associated genes (Table I). Under nitrogen-sufficient conditions, the expression levels of glucosinolate synthesis-associated genes were lower in miRNA transgenic plants than in the wild type, implying that the suppression of *AOP2* by miRNAs mimics nitrogen starvation. Indeed, as shown in Figure 8, several nitrogen starvation-responsive genes were up-regulated in miRNA transgenic plants. A similar negative feedback regulation was reported, in which nitrogen influx increased when Gln synthesis was blocked (Rawat et al., 1999). Given that the loss of function of *AOP2* caused the enhanced nitrogen starvation adaptation, we also compared *mAOP2* transgenic plants with the wild type under nitrogen starvation conditions and found that they showed similar nitrogen starvation adaptation (data not shown), which implied that elevated *AOP2* is not sufficient to raise nitrogen consumption. Plants have evolved diverse mechanisms to adapt to nitrogen starvation conditions. Apparently, reduction of nitrogen consumption and increased nitrogen absorption is an efficient strategy to maintain normal growth and development of plants when nitrogen is unavailable. Our work suggested that *Arabidopsis thaliana* plants have evolved new miRNAs that affect glucosinolate synthesis, leading to improved adaptation to nitrogen starvation conditions.

MATERIALS AND METHODS

Plant Material and Growth Conditions

Arabidopsis thaliana ecotype Cape Verde Islands (Cvi) was used as the wild-type plant in all of our experiments. The seeds were surface-sterilized with 20% bleach and washed three times with sterile water. Sterilized seeds were suspended in 0.1% agarose and plated on Murashige and Skoog (MS) medium. After vernalization for 2 d in the dark at 4°C, the plates were transferred to the culture room at 22°C under a 16-h light/8-h dark photoperiod. For determination of glucosinolate content, 7-d-old seedlings were planted in soil maintained in growth chambers at 22°C and 75% humidity under a 16-h light/8-h dark photoperiod. For observation of root phenotypes, seedlings were grown on vertical MS agar medium containing 0.8% agar. Nitrogen content in the medium was 3 mM (1 mM NH_4NO_3 and 1 mM KNO_3), 0.3 mM (0.1 mM NH_4NO_3 and 0.1 mM KNO_3), and nitrogen free, respectively. To evaluate the seed batch variation, homozygous T3 and T4 generation transgenic plants were respectively used for evaluation of phenotypes.

5′ RACE

Following the manufacturer's instructions for the SMARTer RACE cDNA Amplification Kit (Clontech), 1 μg of total RNA isolated from seedlings grown on nitrogen-free MS medium was used for reverse transcription. Gene-specific primers (designed according to the protocol) and the UPM primer (provided by a kit) were used to conduct PCRs, and purified PCR products were sequenced.

Construct Generation

The putative promoters of *AOP2* were amplified from *Arabidopsis thaliana* (Cvi) genomic DNA using primers Pro-AOP2-F and Pro-AOP2-R (Supplemental Table S1). The fused Pro_{AOP2}-*GUS*-(*m*)*AOP2* was cloned into the pOCA28 vector containing a kanamycin resistance gene. The genomic sequences containing the stem loops of MIR826 or MIR5090 were used as synthetic precursor sequences. The sequences were amplified from *Arabidopsis thaliana* genomic DNA by PCR using primers PremiR826-F, PremiR826-R, PremiR5090-F, and PremiR5090-R (Supplemental Table S1). The PCR products of the precursor sequence were cloned into the pMD18-T vector (http://www.takara.com.cn; Takara) and confirmed by sequencing. The miR826 and miR5090 precursors were subcloned into the pOCA30 vector containing the CaMV 35S promoter. All of the constructs were then transformed into *Agrobacterium tumefaciens* strain GV3101. *Arabidopsis thaliana* transformation was performed by the floral dip method (Clough and Bent, 1998). Transgenic plants were selected using 50 μg/mL kanamycin.

Histochemical GUS Staining

Plant samples were immersed immediately in 1.5 mL staining solution containing 0.5 mg/mL 5-bromo-4-chloro-3-indolyl-β-glucuronic acid (Sigma) in 0.1 M sodium phosphate buffer (pH 7.3). The reaction was performed in the dark at 37°C until a blue-indigo color appeared. After the reaction, seedlings were rinsed in 0.1 M sodium phosphate buffer (pH 7.3). The samples were then rinsed twice in 70% ethanol to remove chlorophylls.

Gene Expression Analysis

For gene expression analysis, plants were grown on MS medium with the indicated nitrogen concentrations for 10 d.

Total RNA was extracted with the Trizol reagent (Invitrogen). Low-M_r RNAs were separated by electrophoresis through denaturing 15% polyacrylamide gels, and miRNA gel-blot hybridizations were performed as described previously (Liang et al., 2010). DNA oligonucleotides complementary to miR826 or miR5090 were end labeled with [α -^{32}P] dATP using T4 polynucleotide kinase and used for hybridizations.

For real-time reverse transcription PCR (RT-PCR), 0.5 μg of total RNA was reverse transcribed using an oligo(dT)$_{18}$ primer (Fermentas) in a 20-μL reaction mixture with RevertAid M-MuLV reverse transcriptase (Fermentas). After heat inactivation, a 1-μL aliquot was used for real-time qRT-PCR. All qRT-PCR analyses were performed using a Lightcycler FastStart DNA Master SYBR Green I kit on a Roche LightCycler real-time PCR machine, according to the manufacturer's instructions. Real-time RT-PCR for miRNAs was detected by stem loop RT-PCR. To produce miRNA-fused stem loop cDNA, 0.5 μg of total RNA was used for the reverse transcription, with miRNA mature sequence-specific stem loop reverse transcription primers designed according to the stem loop RT-PCR protocol (Varkonyi-Gasic et al., 2007). *ACTIN2* (*AT3G18780*) was used as a control for qRT-PCR. The primers used in qRT-PCR are listed in Supplemental Table S1.

Transient Expression in *Nicotiana benthamiana*

Constructs were transformed into *Agrobacterium tumefaciens* strain EHA105 and selected on Luria-Bertani medium containing rifampicin at 50 μg/mL and spectinomycin at 100 mg/L. *Agrobacterium tumefaciens* cells were then infiltrated into leaves of *N. benthamiana*. For coinfiltration experiments, equal volumes of an *Agrobacterium tumefaciens* culture containing *35S:MIR826*, *35S:MIR5090*, or vector (OD_{600} = 1.75) and *35S:(m)AOP2* (OD_{600} = 0.25) were mixed before infiltration into *N. benthamiana* leaves. Leaves were harvested 3 d after infiltration, and total RNA was extracted for small RNA blotting and real-time RT-PCR experiments.

Measurement of Chlorophyll Content

Chlorophyll contents were measured as described by Woodward and Bennett (2005). The pigments from leaves of 10-d-old seedlings were extracted with 5 mL of dimethylformamide for 24 h in the dark at 4°C, and the optical densities (OD_{664} and OD_{647}) for each sample were measured. The chlorophyll content was calculated as follows: ([OD_{664} × 7.04] + [OD_{647} × 20.27]) ×5 / sample weight (in grams) = micrograms chlorophyll/gram fresh weight.

Measurement of Anthocyanin Content

Ten-day-old seedlings grown on MS medium with the indicated nitrogen concentrations were used for anthocyanin analysis. Anthocyanin contents were measured as previously described (Rabino and Mancinelli, 1986). The pigments were extracted from leaves with 99:1 methanol:HCl (v/v) overnight at 4°C. The OD_{530} and OD_{657} for each sample were measured, and $OD_{530} - 0.25 \times OD_{657}$ was used to compensate for the contribution of chlorophyll and its products to the absorption at 530 nm.

Nitrogen Content Analysis

The shoots and roots of plants grown in soil for 4 or 5 weeks were separately harvested and dried at 65°C for 3 d. The samples were milled to a fine powder for nitrogen analysis. Nitrogen analysis was performed using a carbon and nitrogen analyzer (Vario MAX CN; Elementar Analysensysteme).

Glucosinolate Extraction

Glucosinolate extraction was performed as described by Kliebenstein et al. (2001) and Neal et al. (2010). Leaves of 5-week-old wild-type and transgenic plants were harvested, freeze-dried, and then ground to powder. Then 250 mg of the powder was suspended in 5 mL of 70% methanol. After incubation at 70°C for 20 min, 1 mL $Ba(OAc)_2$ (0.4 mol/L) was added and centrifuged at 3000 rpm for 5 min, and the supernatant was added to DEAE-Sephadex A25. The column was then washed twice with water and twice with 1 mL of 20 mM sodium acetate. Sulfatase solution (75 μL), prepared as described by Graser et al. (2000), was then added to the column and left to stand overnight. Desulfonated glucosinolates were eluted in 1-mL aliquots of deionized water and analyzed by ultra-performance liquid chromatography (UPLC)-tandem mass spectrometry.

UPLC-Tandem Mass Spectrometry Analysis of Glucosinolates

Glucosinolate samples were analyzed using a Waters ACQUITY UPLC system and Xevo TQ-S mass spectrometer. Samples (20 $\mu\Lambda$) were separated using an Agilent Zorbax SB-C18 column (4.6 × 250 mm i.d., 5 μm particle size) operated at 1 mL/min at 30°C using the following separation gradient described by Neal et al. (2010): solvent A: H_2O; solvent B: MeCN: 1.5% to 5% (v/v) B (6 min), 5% to 7% (v/v) B (2 min), 7% to 21% (v/v) B (10 min), 21% to 29% (v/v) B (5 min), 29% to 57% (v/v) B (14 min), followed by a cleaning cycle: 57% to 93% (v/v) B (2 min), 5 min hold, 93% to 1. 5% (v/v) B (3 min), 6 min hold. Eluting compounds were monitored at 229 nm. The mass spectral analysis of glucosinolates was obtained with positive electrospray ionization (ESI) in multiple reaction monitoring mode. The ESI source was operated at 4 kV, and the sample cone was operated at 20 V. Nitrogen was used both as bath gas (100°C; 250 L/h) and nebulizing gas (15 L/h). ESI spectra were recorded in the mass range of a 100 to 800 mass-to-charge ratio. Mass spectra of 3-methylsulfinylpropyl, 4-methylsulfinylbutyl, 2-propenyl, and 3-butenyl glucosinolates were analyzed by detecting a single $M+Na^+$ specific for the glucosinolate being tested. 2-propenyl glucosinolate in the samples was further identified with its standard purchased from Sigma-Aldrich.

Sequence data from this article can be found in the GenBank/EMBL data libraries under accession numbers At4g03060 (AOP2), At4g03038 (miR5090), and At4g03039 (miR826).

Supplemental Data

The following materials are available in the online version of this article.

Supplemental Figure S1. Analysis of small RNA sequences.

Supplemental Figure S2. Expression of miRNAs and *AOP2* under nitrogen starvation.

Supplemental Figure S3. Phenotypes of transgenic plants grown on plates.

Supplemental Figure S4. Phenotypes of transgenic plants grown in soil.

Supplemental Figure S5. Nitrogen contents of wild-type and transgenic plants.

Supplemental Table S1. Primers used in this study.

ACKNOWLEDGMENTS

We thank the editor and two anonymous reviewers for their constructive comments, which helped us to improve the manuscript, the Biogeochemical Laboratory and Central Laboratory (Xishuangbanna Tropica Botanical Garden) for their assistance in the determination of nitrogen contents, and the Analytical Instrumentation Center (Kunming Institute of Botany) for UPLC-tandem mass spectrometry analysis of glucosinolates.

Received September 16, 2013; accepted December 22, 2013; published December 23, 2013.

LITERATURE CITED

Abdel-Ghany SE, Pilon M (2008) MicroRNA-mediated systemic down-regulation of copper protein expression in response to low copper availability in *Arabidopsis.* J Biol Chem **283:** 15932–15945

Allen E, Xie Z, Gustafson AM, Carrington JC (2005) microRNA-directed phasing during trans-acting siRNA biogenesis in plants. Cell **121:** 207–221

Allen E, Xie Z, Gustafson AM, Sung GH, Spatafora JW, Carrington JC (2004) Evolution of microRNA genes by inverted duplication of target gene sequences in *Arabidopsis thaliana.* Nat Genet **36:** 1282–1290

Ambros V, Bartel B, Bartel DP, Burge CB, Carrington JC, Chen X, Dreyfuss G, Eddy SR, Griffiths-Jones S, Marshall M, et al (2003) A uniform system for microRNA annotation. RNA **9:** 277–279

Beauclair L, Yu A, Bouché N (2010) microRNA-directed cleavage and translational repression of the copper chaperone for superoxide dismutase mRNA in *Arabidopsis.* Plant J **62:** 454–462

Chen XM (2005) MicroRNA biogenesis and function in plants. FEBS Lett **579:** 5923–5931

Chiou TJ, Aung K, Lin SI, Wu CC, Chiang SF, Su CL (2006) Regulation of phosphate homeostasis by microRNA in *Arabidopsis.* Plant Cell **18:** 412–421

Clough SJ, Bent AF (1998) Floral dip: a simplified method for *Agrobacterium*-mediated transformation of *Arabidopsis thaliana*. Plant J **16:** 735–743

Dai X, Zhao PX (2011) psRNATarget: a plant small RNA target analysis server. Nucleic Acids Res **39:** W155-W159

Fahlgren N, Howell MD, Kasschau KD, Chapman EJ, Sullivan CM, Cumbie JS, Givan SA, Law TF, Grant SR, Dangl JL, et al (2007) High-throughput sequencing of *Arabidopsis* microRNAs: evidence for frequent birth and death of MIRNA genes. PLoS ONE **2:** e219

Fahlgren N, Jogdeo S, Kasschau KD, Sullivan CM, Chapman EJ, Laubinger S, Smith LM, Dasenko M, Givan SA, Weigel D, et al (2010) MicroRNA gene evolution in *Arabidopsis lyrata* and *Arabidopsis thaliana*. Plant Cell **22:** 1074–1089

Felippes FF, Schneeberger K, Dezulian T, Huson DH, Weigel D (2008) Evolution of *Arabidopsis thaliana* microRNAs from random sequences. RNA **14:** 2455–2459

German MA, Pillay M, Jeong DH, Hetawal A, Luo S, Janardhanan P, Kannan V, Rymarquis LA, Nobuta K, German R, et al (2008) Global identification of microRNA-target RNA pairs by parallel analysis of RNA ends. Nat Biotechnol **26:** 941–946

Graser G, Schneider B, Oldham NJ, Gershenzon J (2000) The methionine chain elongation pathway in the biosynthesis of glucosinolates in Eruca sativa (Brassicaceae). Arch Biochem Biophys **378:** 411–419

Grubb CD, Abel S (2006) Glucosinolate metabolism and its control. Trends Plant Sci **11:** 89–100

Hansen BG, Kliebenstein DJ, Halkier BA (2007) Identification of a flavin-monooxygenase as the S-oxygenating enzyme in aliphatic glucosinolate biosynthesis in *Arabidopsis*. Plant J **50:** 902–910

Hsieh LC, Lin SI, Shih AC, Chen JW, Lin WY, Tseng CY, Li WH, Chiou TJ (2009) Uncovering small RNA-mediated responses to phosphate deficiency in Arabidopsis by deep sequencing. Plant Physiol **151:** 2120–2132

Jeong DH, Park S, Zhai J, Gurazada SGR, De Paoli E, Meyers BC, Green PJ (2011) Massive analysis of rice small RNAs: mechanistic implications of regulated microRNAs and variants for differential target RNA cleavage. Plant Cell **23:** 4185–4207

Kant S, Peng M, Rothstein SJ (2011) Genetic regulation by NLA and microRNA827 for maintaining nitrate-dependent phosphate homeostasis in *Arabidopsis*. PLoS Genet **7:** e1002021

Khraiwesh B, Zhu JK, Zhu JH (2012) Role of miRNAs and siRNAs in biotic and abiotic stress responses of plants. Biochim Biophys Acta **1819:** 137–148

Kliebenstein DJ, Lambrix VM, Reichelt M, Gershenzon J, Mitchell-Olds T (2001) Gene duplication in the diversification of secondary metabolism: tandem 2-oxoglutarate-dependent dioxygenases control glucosinolate biosynthesis in *Arabidopsis*. Plant Cell **13:** 681–693

Krapp A, Berthomé R, Orsel M, Mercey-Boutet S, Yu A, Castaings L, Elftieh S, Major H, Renou JP, Daniel-Vedele F (2011) Arabidopsis roots and shoots show distinct temporal adaptation patterns toward nitrogen starvation. Plant Physiol **157:** 1255–1282

Liang G, He H, Yu D (2012) Identification of nitrogen starvation-responsive microRNAs in *Arabidopsis thaliana*. PLoS ONE **7:** e48951

Liang G, Yang FX, Yu DQ (2010) MicroRNA395 mediates regulation of sulfate accumulation and allocation in *Arabidopsis thaliana*. Plant J **62:** 1046–1057

Lu XY, Huang XL (2008) Plant miRNAs and abiotic stress responses. Biochem Biophys Res Commun **368:** 458–462

Maathuis FJ (2009) Physiological functions of mineral macronutrients. Curr Opin Plant Biol **12:** 250–258

Miller AJ, Fan X, Shen Q, Smith SJ (2008) Amino acids and nitrate as signals for the regulation of nitrogen acquisition. J Exp Bot **59:** 111–119

Miller AJ, Shen Q, Xu G (2009) Freeways in the plant: transporters for N, P and S and their regulation. Curr Opin Plant Biol **12:** 284–290

Neal CS, Fredericks DP, Griffiths CA, Neale AD (2010) The characterisation of AOP2: a gene associated with the biosynthesis of aliphatic alkenyl glucosinolates in *Arabidopsis thaliana*. BMC Plant Biol **10:** 170

Palatnik JF, Allen E, Wu XL, Schommer C, Schwab R, Carrington JC, Weigel D (2003) Control of leaf morphogenesis by microRNAs. Nature **425:** 257–263

Pant BD, Musialak-Lange M, Nuc P, May P, Buhtz A, Kehr J, Walther D, Scheible WR (2009) Identification of nutrient-responsive Arabidopsis and rapeseed microRNAs by comprehensive real-time polymerase chain reaction profiling and small RNA sequencing. Plant Physiol **150:** 1541–1555

Peng MS, Bi YM, Zhu T, Rothstein SJ (2007) Genome-wide analysis of *Arabidopsis* responsive transcriptome to nitrogen limitation and its regulation by the ubiquitin ligase gene *NLA*. Plant Mol Biol **65:** 775–797

Rabino I, Mancinelli AL (1986) Light, temperature, and anthocyanin production. Plant Physiol **81:** 922–924

Rajagopalan R, Vaucheret H, Trejo J, Bartel DP (2006) A diverse and evolutionarily fluid set of microRNAs in *Arabidopsis thaliana*. Genes Dev **20:** 3407–3425

Rawat SR, Silim SN, Kronzucker HJ, Siddiqi MY, Glass AD (1999) AtAMT1 gene expression and NH4+ uptake in roots of *Arabidopsis thaliana*: evidence for regulation by root glutamine levels. Plant J **19:** 143–152

Remans T, Nacry P, Pervent M, Filleur S, Diatloff E, Mounier E, Tillard P, Forde BG, Gojon A (2006a) The *Arabidopsis* NRT1.1 transporter participates in the signaling pathway triggering root colonization of nitrate-rich patches. Proc Natl Acad Sci USA **103:** 19206–19211

Remans T, Nacry P, Pervent M, Girin T, Tillard P, Lepetit M, Gojon A (2006b) A central role for the nitrate transporter NRT2.1 in the integrated morphological and physiological responses of the root system to nitrogen limitation in Arabidopsis. Plant Physiol **140:** 909–921

Sønderby IE, Geu-Flores F, Halkier BA (2010) Biosynthesis of glucosinolates—gene discovery and beyond. Trends Plant Sci **15:** 283–290

Tsay YF, Ho CH, Chen HY, Lin SH (2011) Integration of nitrogen and potassium signaling. Annu Rev Plant Biol **62:** 207–226

Varkonyi-Gasic E, Wu R, Wood M, Walton EF, Hellens RP (2007) Protocol: a highly sensitive RT-PCR method for detection and quantification of microRNAs. Plant Methods **3:** 12

Vidal EA, Gutiérrez RA (2008) A systems view of nitrogen nutrient and metabolite responses in *Arabidopsis*. Curr Opin Plant Biol **11:** 521–529

Voinnet O (2009) Origin, biogenesis, and activity of plant microRNAs. Cell **136:** 669–687

Wang JW, Wang LJ, Mao YB, Cai WJ, Xue HW, Chen XY (2005) Control of root cap formation by MicroRNA-targeted auxin response factors in *Arabidopsis*. Plant Cell **17:** 2204–2216

Wang YY, Hsu PK, Tsay YF (2012) Uptake, allocation and signaling of nitrate. Trends Plant Sci **17:** 458–467

Wentzell AM, Rowe HC, Hansen BG, Ticconi C, Halkier BA, Kliebenstein DJ (2007) Linking metabolic QTLs with network and cis-eQTLs controlling biosynthetic pathways. PLoS Genet **3:** 1687–1701

Wittstock U, Halkier BA (2002) Glucosinolate research in the *Arabidopsis* era. Trends Plant Sci **7:** 263–270

Woodward AJ, Bennett IJ (2005) The effect of salt stress and abscisic acid on proline production, chlorophyll content and growth of in vitro propagated shoots of *Eucalyptus camaldulenis*. Plant Cell Tissue Organ Cult **82:** 189–200

Wu G, Park MY, Conway SR, Wang JW, Weigel D, Poethig RS (2009) The sequential action of miR156 and miR172 regulates developmental timing in *Arabidopsis*. Cell **138:** 750–759

Yang JH, Han SJ, Yoon EK, Lee WS (2006) 'Evidence of an auxin signal pathway, microRNA167-ARF8-GH3, and its response to exogenous auxin in cultured rice cells'. Nucleic Acids Res **34:** 1892–1899

Yamasaki H, Abdel-Ghany SE, Cohu CM, Kobayashi Y, Shikanai T, Pilon M (2007) Regulation of copper homeostasis by micro-RNA in *Arabidopsis*. J Biol Chem **282:** 16369–16378

Yogeeswaran K, Frary A, York TL, Amenta A, Lesser AH, Nasrallah JB, Tanksley SD, Nasrallah ME (2005) Comparative genome analyses of *Arabidopsis* spp.: inferring chromosomal rearrangement events in the evolutionary history of *A. thaliana*. Genome Res **15:** 505–515

Yuan L, Loqué D, Kojima S, Rauch S, Ishiyama K, Inoue E, Takahashi H, von Wirén N (2007) The organization of high-affinity ammonium uptake in *Arabidopsis* roots depends on the spatial arrangement and biochemical properties of AMT1-type transporters. Plant Cell **19:** 2636–2652

Zhang H, Forde BG (1998) An *Arabidopsis* MADS box gene that controls nutrient-induced changes in root architecture. Science **279:** 407–409

Zhao M, Ding H, Zhu JK, Zhang F, Li WX (2011) Involvement of miR169 in the nitrogen-starvation responses in *Arabidopsis*. New Phytol **190:** 906–915